Chapter 1

Diffraction Gratings in Composite Materials

Introduction

The particular case of scattering of light which is commonly referred to as diffraction is extremely interesting when diffraction gratings are considered. A diffraction grating can be defined as a device able to scatter the impinging light in a 'ordered' way, that is, in a limited amount of directions. This behavior is due to the fact that a diffraction grating exhibits a periodic spatial modulation of its dielectric constant. When a light wave impinges on the grating, this modulation induces an effect of mutual interference between the different parts of the wavefront; only at particular angles this interference will be constructive and the macroscopic effect will be a deflection of the original wave in several directions, which are often referred to as diffracted orders. When dealing with diffraction gratings, a main classification can be made, depending whether they operate in the Raman-Nath or in the Bragg regime. The first one applies to gratings which divide the impinging beam in multiple diffracted orders; they are commonly called *thin gratings*. In the case of Bragg regime, also called "volume" or *thick gratings*, the impinging beam is divided only into a single diffracted beam in addition to a partially transmitted one; in this case the Bragg condition for wave-vectors holds.

An exact distinction between thin and thick gratings can be found in the work by Gaylord and Moharam[1]. One of the most useful optical parameter to measure the quality of a diffraction grating is the diffraction efficiency (η). We define diffraction efficiency as the ratio of the intensity of the desired diffracted beam and the intensity of the incidence beam. Diffraction efficiency $\eta = f(\theta_{inc}, \lambda, d, \Delta n)$ is a function of the incidence angle, wavelength, grating depth, index modulation. By optimizing these parameters it is possible to obtain grating structures with high value of diffraction efficiency.

1.1 Thin and thick gratings

The terminology *thin* and *thick* gratings is widely used. However, these terms frequently either are not defined, vaguely defined, or defined in an ambiguous way. Interpretations of *thin* and *thick* grating behavior appear in the literature dating back to the 1930's. These interpretations with their various degrees of preciseness and accuracy have been carried forward in parallel in many cases. The terminology of *thin* and *thick* gratings is often confusing to workers in fields that use planar gratings (such as acoustooptics, holography, integrated optics, and spectroscopy). The purpose of this short introduction is to clarify the possible practical explicit definitions of *thin* and *thick* gratings. This is done in terms of the diffraction regime characteristics and angular and wavelength selectivity characteristics of the grating. For brevity, only the common case of planar gratings with grating fringes perpendicular to the surfaces is discussed. For a plane wave incident upon a planar grating with sinusoidal permittivity fringes normal to the surface, the fields inside the grating may be completely described by the rigorous coupled-wave equations[2].

These equations are obtained by substituting the periodic relative permittivity, the plane wave field expansion, and the Floquet theorem into the wave equation. For H-mode polarization the result is:

$$\frac{1}{2\pi}\frac{d^2 S_i(z)}{dz^2} - j\frac{2(\varepsilon_0)^{1/2}\cos\theta}{\pi\lambda}\frac{dS_i(z)}{dz} + \frac{2i(m-i)}{\Lambda^2}S_i(z) + \frac{\varepsilon_1}{\lambda^2}[S_{i+1}(z) + S_{i-1}(z)] = 0 \quad (1)$$

where $S_i(z)$ are the fields inside the grating, i is the (integer) order of diffraction, ($-\infty < i < +\infty$), ε_0 is the average relative permittivity, ε_1 is the amplitude of the sinusoidal relative permittivity, λ is the free space wavelength, θ is the angle of refraction of the incident wave, Λ is the grating period, and m is given by

$$m\lambda/(\varepsilon_0)^{1/2} = 2\Lambda\sin\theta \quad\quad\quad (2)$$

This is a Bragg condition when *m* is an integer. Equation (1) is derived without approximation. The Raman-Nath diffraction regime may be obtained from Eq. (1) by neglecting the $d^2 S_i/dz^2$ and S_i terms. The Bragg diffraction regime may be obtained from Eq. (1) by neglecting the $d^2 S_i/dz^2$ term and considering only *i* = 0,1. This corresponds to the Kogelnik two-wave coupled-wave theory. In any case, the diffraction efficiency is given by $\eta_i = S_i S_i^*$ for unslanted phase gratings.

A *thin* grating may be described as a grating that produces Raman-Nath regime diffraction.2 In this case, the multiple grating diffracted-orders ideally have diffraction efficiencies η_i given by

$$\eta_i = J_i^2(2\gamma) \quad\quad\quad (3)$$

where i is the integer representing the diffracted-order, J_i is an integer-order ordinary Bessel function of the first kind, and γ is the grating strength parameter given by $\gamma = \pi\varepsilon_1 d/(\varepsilon_0)^{1/2}\Lambda^2\cos\theta$, and *d* is the grating thickness.

A *thick* grating (or *volume* grating) may be described as a grating that produces Bragg regime (or two-wave regime) diffraction. This is described by the two-wave coupled-wave theory of Kogelnik. In this regime, the single fundamental diffracted-order ideally has a diffraction efficiency given by

$$\eta_i = \sin^2 \gamma \qquad (4)$$

For E-mode polarization the y in Eq. (4) is $\gamma = \pi \varepsilon_1 d \cos(2\theta) / 2\lambda(\varepsilon_0)^{1/2} \cos\theta$ We can compare in the following graph the first order diffraction efficiencies for Raman-Nath (thin grating) regime and for Bragg (thick grating) regime.
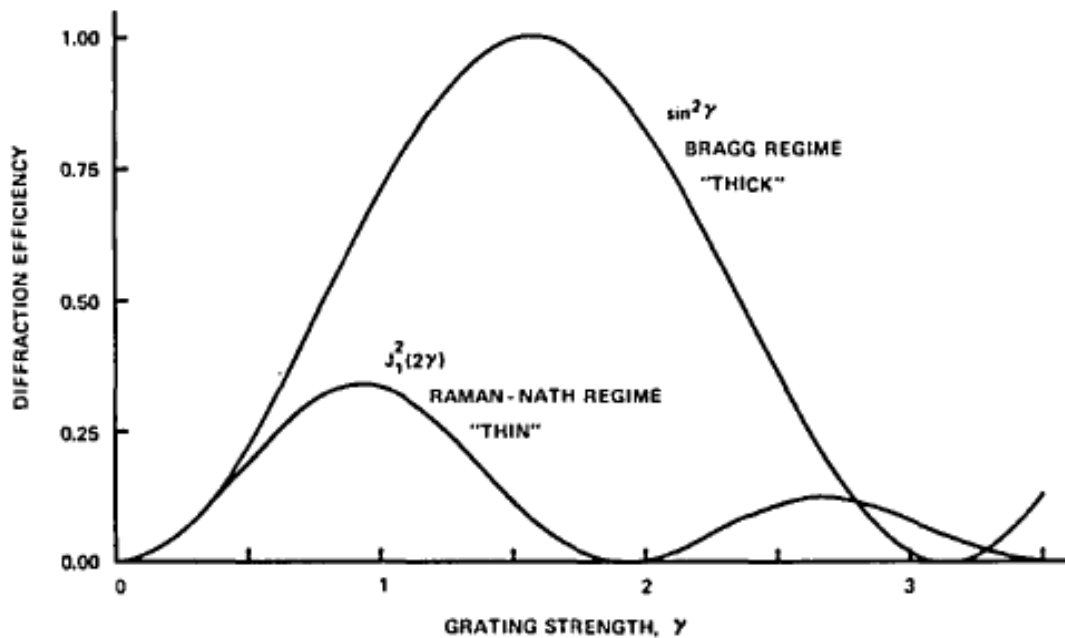

Figure 1.1: Ideal first-order diffraction efficiencies for Raman-Nath and Bragg regime.

A *thin* grating may be alternatively described as a grating exhibiting relatively little angular and wavelength selectivity. As the incident wave is dephased (either in angle incidence or in wavelength) from the Bragg condition, the diffraction efficiency decreases.

The angular range or wavelength range for which the diffraction efficiency decreases to half of its on-Bragg-angle value is determined by the thickness of the grating *d* expressed as a number of grating periods Λ. For a *thin* grating this number may be reasonably chosen to be

$$d/\Lambda < 10 \tag{5}$$

The region of *thin* grating behavior according to the angular and wavelength-selectivity-based definition (5) is depicted in Fig. 1.2.
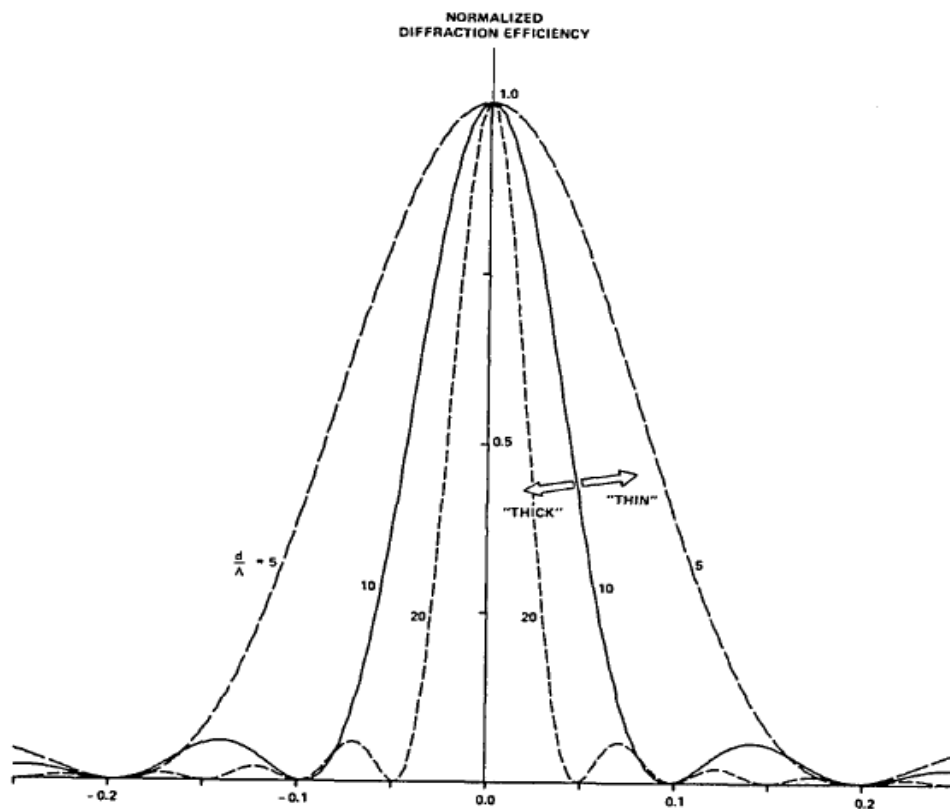
Figure 1.2: Typical angular selectivity plots for various values of d/Λ.

Gratings having angular and wavelength selectivities with FWHM wider than that for d/Λ=10 may be considered to be *thin* gratings. This definition does not accurately predict the diffraction regime. It has the desirable feature that the governing parameter *(d/Λ)* is directly proportional to the grating thickness, and thus *thin* and *thick* have direct physical interpretations.

A thick grating may conversely be described as a grating exhibiting strong angular and wavelength selectivity. A relatively small change in the angle of incidence from the Bragg angle or a relatively small change in the wavelength at the Bragg angle produces significant dephasing and the diffraction efficiency decreases correspondingly. *Thick* grating behaviour may be considered to occur when

$$d/\Lambda > 10 \tag{6}$$

This is the angular-and-wavelength-selectivity-based definition of a *thick* grating. The region of this behavior is also shown in Fig. 1.2.

1.2 Holographic Diffraction Grating

Around 1947, scientist Dennis Gabor developed the theory of holography while working to improve the resolution of an electron microscope. A holograph is an image made by exposing a photosensitive film to the interference pattern created when two (or more) laser light sources shine on an object. A *diffraction grating* is a collection of reflecting (or transmitting) elements separated by a distance comparable to the wavelength of light under study. It may be thought of as a collection of diffracting elements, such as a pattern of transparent slits (or apertures) in an opaque screen, or a collection of reflecting grooves on a substrate. When two sets of coherent polarized optical plane waves of equal intensity intersect each other, a standing wave pattern will be formed in the region of intersection if both sets of waves are of the same wavelength (Fig 1.3). The combined intensity distribution forms a set of straight equally- spaced fringes (bright and dark lines). We show in figure 1.3 a typical interference pattern:
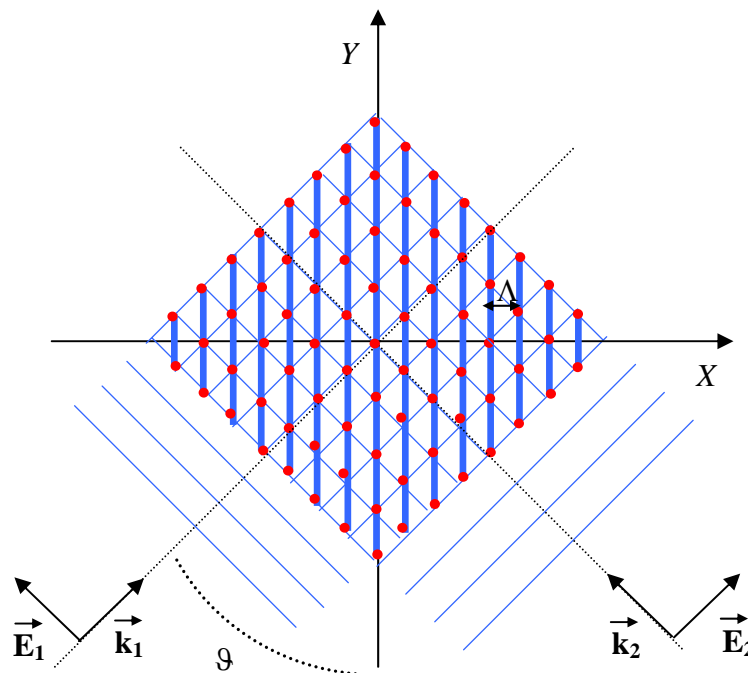
Figure 1.3: Interference pattern generated by the overlap of two plane waves. E_1, E_2 are the amplitude of electric field, K is the wave vector, ϑ is half angle between the beams, Λ is the distance between two adjacent fringes

We can represent the same geometry in the wave vector space like:
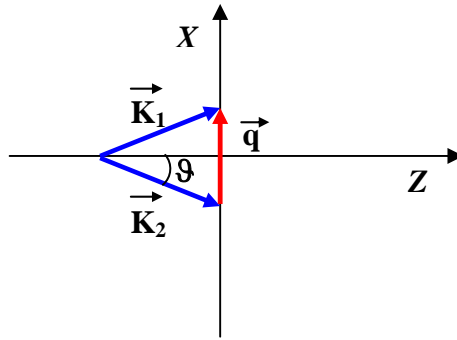
Figure 1.4: Realization of a interference pattern with two plane waves of wave vector $\mathbf{K_1}$, $\mathbf{K_2}$

Considering Fig 1.4, the total electric field due to interference of the two waves will be:

$$E_{tot}(r,t) = E_1 \exp(i(k_1 \cdot r - \omega t)) + E_2 \exp(i(k_2 \cdot r - \omega t))$$

Where, E_1 and E_2 are the amplitudes of the electric field, k_1 and k_2 are the wave vectors of the two waves plane and ω is the frequency. The intensity of this field will be $W \propto \mathbf{E}_{tot} \cdot \mathbf{E}_{tot}^*$, namely:

$$W = W_0(1 + m\cos qx) \qquad (6)$$

Where $m = 2\dfrac{\sqrt{I_1 I_2}}{I_1 + I_2}$ represents the fringe visibility of the grating (if the intensities of the two beams are the same, m=1), $W_0 = I_1 + I_2$, $\mathbf{q} = \mathbf{k_1} - \mathbf{k_2}$ is the wave vector of the interference pattern. The fringe visibility m, is a key parameter during the grating formation. We will see in the next paragraphs the importance of this parameter. The spatial periodicity Λ is:

$$\Lambda = \frac{2\pi}{q}$$

Where q=|**q**|. From figure 4 it is possible to see $q = 2k \sin\left(\dfrac{\vartheta}{2}\right)$, with k=| **k₁**|=|**k₂**|. Now it is possible to relate Λ with the wavelength of the incidence radiation

$$\Lambda = \frac{\lambda}{2\sin\vartheta} \qquad (7)$$

and ϑ is half the angle between the beams. A small angle between the beams will produce a widely spaced fringe pattern (large Λ), whereas a larger angle will produce a fine fringe pattern. The lower limit for Λ is $\lambda/2$, so for visible recording light, thousands of fringes per millimeter may be obtained. The combined intensity (6) varies sinusoidally with position as the interference pattern is scanned along a line. Various optical gratings, can be realized, in a holographic way, by recording the interference pattern on different recording materials.

1.3 Optical Holographic Setup

Interferometric techniques have become extremely useful tools in many fields of modern science and technology, and have been applied to various applications such as recording image holograms, making holographic optical elements, precision metrology, etc. Most of these applications require extremely stable interference patterns. Consequently, scientists and engineers have developed both passive and active techniques to stabilize these patterns. This problem becomes critical when the realization of holographic diffraction gratings by UV curing techniques is concerned. In particular, when a holographic exposure takes more than a small fraction of a second, even fluctuations in the index of refraction of the air traversed by interfering laser beams, as well as vibrations and thermal drifts, can introduce changes in the optical path-length difference between the beams. It can be easily shown that these changes lead to motion in the interference pattern, which degrades the contrast in the resulting exposure.

But there are also other technical factors that can induce a fluctuation of the "optical path length difference":

- Laser wavelength shift or mode hopping due to instability in the laser cavity.
- Optical table warping due to improper balancing or slow air leakage in the pneumatic suspension legs.
- Movement of mechanical components holding beam forming optical elements due to mechanical vibrations transmitted through the floor, acoustic noise tranmitted through the air and from thermal expansion and contraction.
- Local air density variations due to turbulence, temperature and humidity drift.
- Thermal expansion or contraction of optical elements due to changes in room temperature.
- Thermal expansion of optical components such as lenses and mirrors due to the heat generated by recording laser beams.

This long list underlines the importance of this problem. There are however several ways to solve it. One consists in removing any possible source of noise. This can be obtained by adopting reinforced post and mounts and using an antivibration table with an autoleveling pneumatic system. To improve fringe contrast also ambient light must be eliminated. Thermal gradients and air flows, which change the local index of refraction in the beams of the interferometer, must be avoided. During the recording process, the components of the optical system must be extremely clean, and mirrors, pinholes and spatial filters must be adjusted as carefully as possible. In order to clean the beam profile of the impinging beam a standard spatial filter is necessary. It is composed by a lens followed by a small aperture in the focus, and then the beam can be collimated with another lens.
Any object in the optical system receiving laser illumination, even a grain of dust, may scatter light toward the grating contributing to stray light.

1.4   POLICRYPS holographic gratings

Among the most spread and investigated liquid crystalline composite materials there are Polymer-Dispersed Liquid Crystals (PDLCs). Since the late 80's, PDLCs have attracted a wide interest, both from the scientific community, for the aspects of the related basic research, and from industries due to the technological relevance of these systems for display and window technology[3]. In a PDLC material, liquid crystal (LC) filled cavities (droplets) are randomly distributed within a rigid polymer matrix[4]. The possibility of realizing electrically driven diffraction gratings based on Liquid Crystalline composite materials was first pointed out by Margerum and coworkers in late '80[5,6] The works of Sutherland et. al. in early 90[7,8] started to investigate the utilization of Polymer Dispersed Liquid Crystals (PDLC)-based gratings as new systems for fabricating electrically switchable diffraction and holographic devices (usually referred to as holographic PDLC, or H-PDLC). The optical properties of H-PDLC devices strongly depend on the presence of LC droplets inside the gratings. In the case of conventional H-PDLCs we have, in general, low switching voltages but rather large droplet sizes. This constitutes a dramatic drawback related to the optical scattering of light. A possibility to overcome the problem is represented by nano-sized H-PDLCs. They present low scattering losses but, on the other hand, high switching voltages. Recently, an attempt has been made to fabricate a new kind of holographic gratings which could exploit this method[9] nd new intriguing morphologies have been realized. These gratings consist of polymer slices alternated to films of regularly aligned NLC (we proposed to call them POLICRYPS, acronym of POlymer LIquid CRYstal Polymer Slices).

Besides the particular degree of quality of the obtained morphology, a further confirm of the absence of NLC droplets in the POLICRYPS structure is reported in Fig.1.5 where it is shown the presence of disclination defects inside fringes occupied by NLC molecules. This kind of texture defects are usually pertinent only to well aligned liquid crystal films.
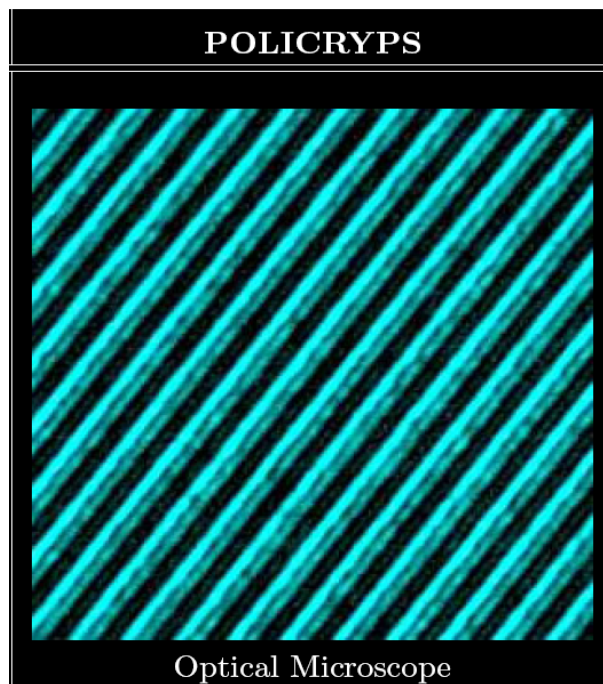

Figure 1.5: Optical morphology of a POLICRYPS grating obtained by using an optical microscope

The basic idea for the fabrication of POLICRYPS is to avoid the formation of a separate NLC phase during the curing process; in this way, we avoid the growing of NLC droplets obtaining, on the contrary, only a macroscopic phase separation, that is to say, an almost complete re-distribution of nematic and monomer components inside the sample. This result is obtained by exploiting the high diffusion which the NLC molecules can undergo when they are in the isotropic state; the realization of POLICRYPS gratings is therefore the result of a new technique, that we have introduced, and called MPTIPS, from the acronym Mixed Polymerisation Thermal Induced Phase Separation.

The standard procedure consists of the following steps[9]:

a) The heating of a sample of photoinitiator - monomer - NLC mixture up to a temperature which is above the Nematic-Isotropic transition point of the NLC component. This step prevents the appearance of a nematic phase during the curing process;

b) The illumination of the sample with the interference pattern of a curing UV radiation;

c) The slow cooling of the sample below the Isotropic-Nematic transition point (typically, down to the room temperature) after the curing radiation has been switched off and the polymerization process has come to an end.

The general procedure to obtain POLICRYPS gratings is resumed in Fig. 1.6
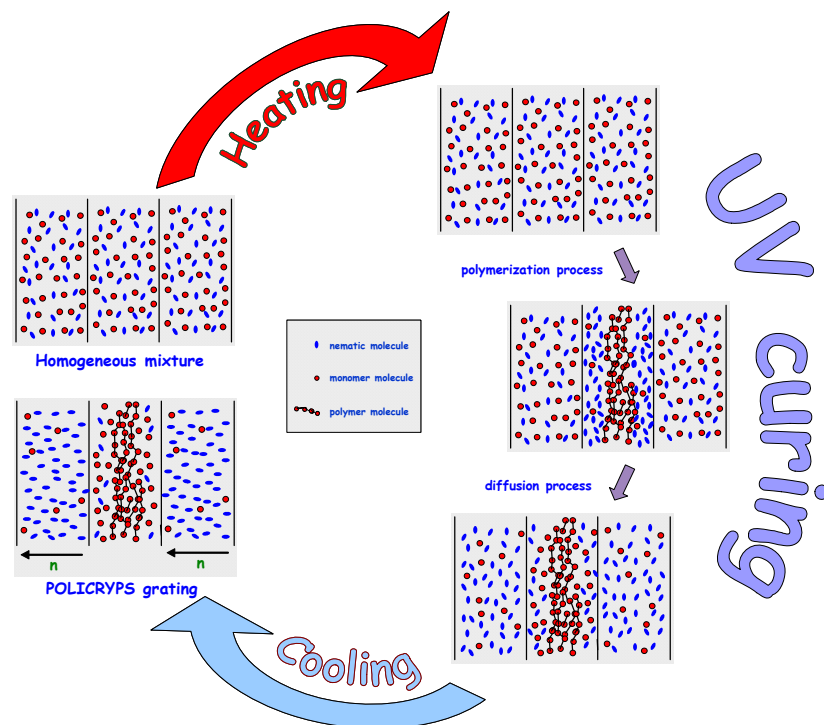
Figure 1.6: Sketch of POLICRYPS gratings production procedure. The diffusion of the involved species is improved by the simple trick of curing the gratings at a temperature which is above the N-I transition point of the used liquid crystal material.

1.5 Comparison between H-PDLC and POLICRYPS gratings

We report now a comparison between the performances of PDLC and POLICRYPS gratings. Two sample cells have been prepared in which a PDLC and a POLICRYPS grating were realized starting from the same initial chemical mixture. The experimental set-up used presented in Fig.7: it is a typical setup for the UV curing process and diffraction efficiency measurement. The light from an Ar-ion laser (λ_B = 0.351 μm) is broadened by a beam expander and split into two beams (of nearly the same intensity) which provide an interference pattern when intersecting in the plane of the tunable aperture I. In this geometry, the interference angle θ_{cur} can be easily varied in the range 1°÷60°; therefore the spatial period Λ of our gratings can be varied approximately in the range 0.2 μm – 11 μm. Measurements reported in this comparison have been made on a PDLC and a POLICRYPS grating both with Λ = 1.5 μm obtained by using an interference angle θ_{cur} = 6.7°. The temperature of the sample is monitored by a thermo-stage.
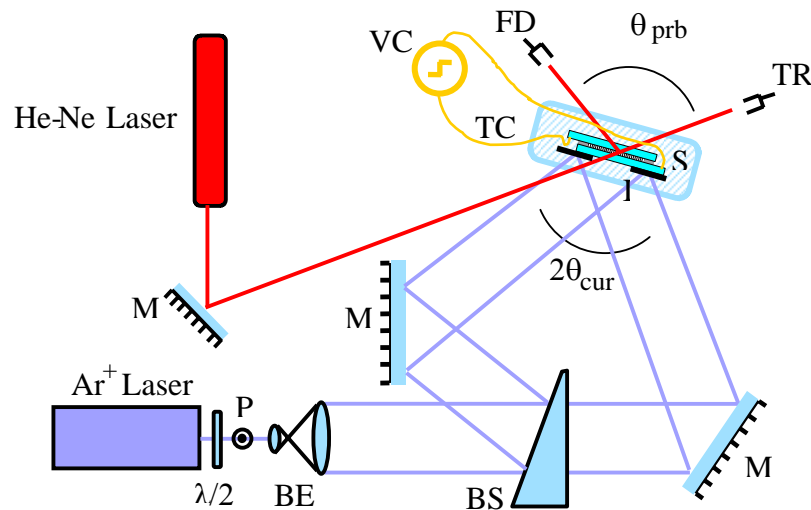

Figure 1.7: Optical setup for UV curing of gratings and their diffraction efficiency measurement. *P*, polarizer; *λ/2*, half-wave plate; *BE*, beam expander; *BS*, beam splitter; *2θcur*, total curing angle; *2θprb*, incidence angle of the probe beam; *M*, mirrors; *TC*, thermo-controller stage; *I*, tunable aperture; *S*, sample; *FD*, first-order diffracted photo-detector; *TR*, transmitted order photo-detector.

The measuring part of the set-up utilizes a weak ($\approx$ 1 mW), He-Ne laser radiation (λ_R = 0.633 μm), which is exploited as a "probe" beam; its angle of incidence is adjusted for satisfying the Bragg condition for the 1st order diffracted beam. For each sample, before starting the curing process, the intensity I_{in} of the impinging beam (before the sample) and the transmitted intensity I_{tr} are measured. Then, once the curing process has been completed and the UV light switched off, also the intensity I_0 of the zero order (directly transmitted) probe beam and the intensity I_1 of the first order diffracted beam are measured. In this way the zero order transmittivity $T_0 = I_0 / I_{in}$, the first order transmittivity $T_1 = I_1 / I_{in}$, the total transmittivity $T_{Tot} = T_0 + T_1$ and the first order diffraction efficiency, $\eta_1 = I_1 / I_{tr}$ can be obtained.

The chemical mixture used to fill the cells has been prepared by diluting a small amount of 5CB NLC ($\approx$30 wt %) in the pre-polymer system Norland Optical Adhesive NOA-61; the sample cells, made by using indium tin oxide-coated glass slabs, were 16 μm thick. The POLICRYPS grating has been cured by a total UV intensity of 11 mW/cm^2, acting on the sample for $\approx$ 1000 sec., these being the optimal conditions for achieving a high diffraction efficiency and a morphology of good quality[10,11]. Indeed, not only a longer exposure does not produce any modification of the grating, but also post-curing treatments with uniform UV exposure are absolutely ineffective. Almost the same UV intensity and curing time proved to be adequate for producing a PDLC grating too.

During all the measurements, the intensity of the probe beam was maintained at a fixed value (the value of the initial impinging intensity before the curing process started). We have deduced the first order diffraction efficiency at room temperature both for POLICRYPS and PDLC gratings, obtaining $\eta_1^{POLICRYPS}$ = 88% and η_1^{PDLC} = 41.2%. Although the value $\eta_1^{POLICRYPS}$ is quite high, it is not the highest that we have got; with different POLICRYPS gratings (not comparable with PDLC ones) we have got values as high as 98%.

The electro-optic response of the two gratings has been investigated by exploiting a low frequency (500 Hz) square wave voltage, and the results are reported in Fig. 1.8. Fig. 1.8a represents the switching curve of the POLICRYPS grating: the behaviour of the first order transmittivity T_1 (circles), zero order transmittivity T_0 (squares) and total transmittivity T_{Tot} (triangles) is reported versus the applied electric field. We note that T_{Tot} is only slightly less than 1 and remains approximately the same for all the values of the applied field. This indicates that the grating presents negligible scattering losses. The situation is quite different for the PDLC grating (Fig. 1.8b): the total transmittivity is well below 1 and increases as the applied voltage increases. We also note that, although the residual diffracted transmittivity of the POLICRYPS grating after the field is switched off is higher than that of the H-PLDC, the switching efficiency $h_{sw} \equiv \left(T_1^{on} - T_1^{off} \right) / T_1^{on}$, where T_1^{on} and T_1^{off} are the first order transmittivity in the switch-on and switch-off conditions, respectively, is the same (93.3 %) for both gratings.

(a)   (b)
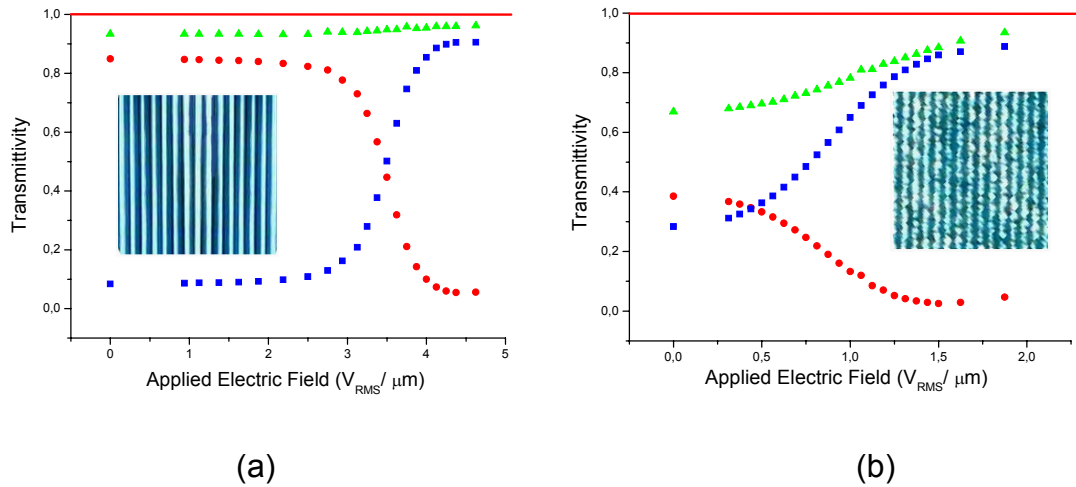
Figure 1.8. Applied field dependence of zero-order transmittivity T_0 (squares), first-order transmittivity T_1 (circles), and total transmittivity T_{tot} (triangles) for (a) a POLICRYPS grating and (b) a PDLC grating at room temperature. Error bars are of the order of the symbol size. The insets show typical (a) POLICRYPS and (b) PDLC grating morphology with the same spatial period, observed under a polarizing optical microscope.

As far as the switching voltages are concerned, the first diffracted beam is almost completely switched off by a field of about 1.5 V/μm, whereas a value of about 4.3 V/μm is needed to obtain the same effect in the POLICRYPS grating. This particular difference can be attributed to the average size of NLC droplets in the PDLC grating; evidently, they are large enough to make possible low switching fields. This result is confirmed by the switching times resumed in table 1.

	τ_{fall} (ms)	τ_{rise} (ms)
POLICRYPS	$1,12 \pm 0,03$	$0,88 \pm 0,03$
PDLC	$10,53 \pm 0,18$	$1,36 \pm 0,04$

Table 1. Measured switching times for a POLICRYPS and
a PDLC grating obtained from the same initial mixture

Both rise and fall times of the PDLC grating are longer than those of the POLICRYPS; this suggests a very large (1 mm) average size of PDLC droplets. On the other hand, the higher switching fields needed to switch the POLICRYPS gratings can be explained in terms of the presence of a thin hybrid layer at the interface between NLC films and polymeric slices; in this layer some polymeric interconnections can strongly increase the local viscosity and hamper the alignment of the NLC molecules; investigations in this direction are under way.